INTERNATIONAL SOCIETY FOR
SOIL MECHANICS AND
GEOTECHNICAL ENGINEERING

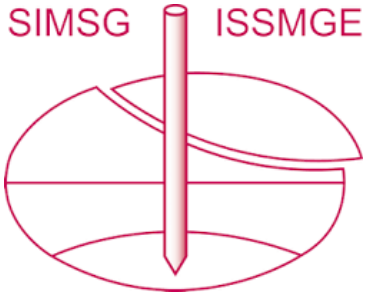

This paper was downloaded from the Online Library of the International Society for Soil Mechanics and Geotechnical Engineering (ISSMGE). The library is available here:

https://www.issmge.org/publications/online-library

This is an open-access database that archives thousands of papers published under the Auspices of the ISSMGE and maintained by the Innovation and Development Committee of ISSMGE.

3D Numerical Analysis of a Suspension Bridge Anchor Block to Oblique-Slip Fault Movement

Analyse numérique 3D d'un bloc d'ancrage de pont suspendu soumis à un mouvement oblique de glissement dû à une faille de rupture

Avar B.B.
Flint & Neill Ltd, a COWI Group Company, London, United Kingdom
Augustesen A.H., Kasper T., Steenfelt J.S.
COWI A/S, Kongens Lyngby, Denmark

ABSTRACT: The paper presents results from 3D finite element (FE) analysis of the response of a suspension bridge anchor block to oblique-slip fault movement. The study attempts to understand the behaviour of the bridge anchor block in terms of displacements and stresses acting on the block as a result of fault movement in order to assess the robustness of the structure. The fault displacements result in minor changes in horizontal stresses acting on the anchor block vertical faces. Due to the rotational displacement effect of the vertical fault displacement an uneven vertical stress distribution at the bottom of the anchor block can be observed. The rotation and translation of the anchor block have been evaluated to be within acceptable limits.

RÉSUMÉ : Ce document présente les résultats de l'analyse 3D aux éléments finis de la réponse d'un bloc d'ancrage de pont suspendu à un mouvement oblique de glissement dû à une faille. L'étude vise à appréhender le comportement du bloc d'ancrage du pont, du point de vue des déplacements et des efforts appliqués, résultant du mouvement de faille, afin de déterminer la robustesse de la structure. Les mouvements de faille n'ont que peu d'incidence sur les efforts horizontaux appliqués aux faces verticales du bloc d'ancrage. Toutefois, en raison de l'effet rotationnel engendré par les déplacements verticaux de la faille, on observe une distribution plus inégale des efforts verticaux à la base du bloc d'ancrage. La rotation et les déplacement de ce dernier ont été calculés afin d'être dans des limites acceptables.

KEYWORDS: Anchor block, suspension bridge, fault rupture, soil/structure interaction, FE analysis.

1 INTRODUCTION

The type of foundations used for structures such as bridges affect the performance of the structure during faulting (Gazetas et al. 2008). In recent years comprehensive studies including field observation and numerical analysis supported by centrifuge model tests have been conducted to develop a methodology to analyse and design foundation/structure systems against fault rupture (e.g. Gazetas et al. 2007, Faccioli et al. 2008, Anastopoulos et al. 2008, Loli et al. 2012).

The studies show that the presence of the structure, depending on the rigidity of its foundation, can divert the rupture path as opposed to free-field fault outcropping. Furthermore, depending on the relative rigidity of the foundation with respect to the soil, the foundation and the structure experience differential displacements and rotations different from those of the free-field ground surface.

Massive concrete anchor blocks are often used to anchor the suspension bridge main cables which carry the bridge deck. In this paper, the impact of oblique-slip fault movements passing under a massive gravity anchor block in terms of displacements and stresses have been investigated using 3D finite element (FE) analysis. The behaviour of the anchor block-soil interaction has been compared with free-field fault movements.

2 PROJECT DESCRIPTION

The anchor block analysed in this paper was the initial solution for a suspension bridge crossing the Izmit Bay in Turkey, which is to be located southeast of Istanbul. The free span of the bridge is 1550 m in length with two 566 m long side spans. The anchor block is located at the south end of the bridge. The site investigation proved the presence of secondary fault systems under the anchor block.

3 NUMERICAL MODELING

The anchor block is located in a multi-layered soil medium. The fault plane is situated at the base of the soil medium representing the interface between soil and rigid bedrock. It is assumed that vertical and lateral movements may occur simultaneously creating an oblique-slip faulting.

Numerical modelling using PLAXIS 3D 2011 FE software is adopted. The size of the model is 500 x 1400 x 130 m (see Fig. 1).

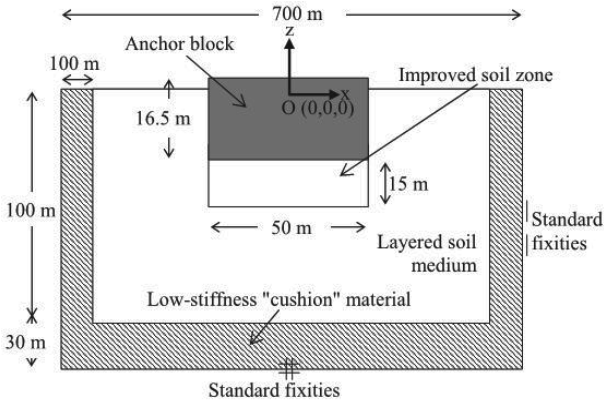

Figure 1. Indicative cross section showing the anchor block and the model dimensions.

To reduce the effect of the outer boundaries of the soil volume as well as to ensure sufficient calculation accuracy and to correctly apply the fault displacements, an artificial low-stiffness "cushion material" is placed around the soil medium. This zone allows the general standard fixities in PLAXIS to be introduced at the outer boundaries of the cushion material. The unit weight of the cushion material is the same as the soil

leading to reasonable stresses acting on the soil medium at the in-situ stress calculation phase.

3.1 *Anchor block*

A simplified model has been used to create the massive foundation block and the improved soil zone beneath it (see Fig. 2). The massive foundation block of the anchor has been modelled using linear elastic (non-porous) material continuum elements. The loads acting on the anchor block are shown in Fig. 2.

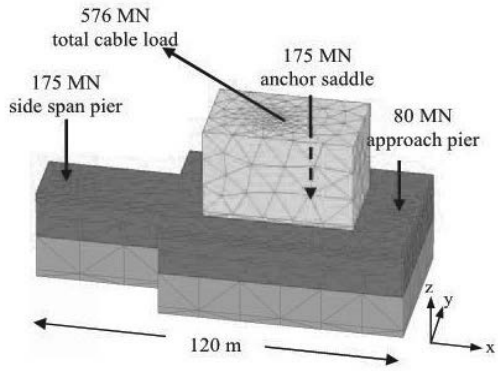

Figure 2. Anchor block model in PLAXIS 3D and structural loads.

The zone beneath the massive foundation improved by bored piles has been modelled as an equivalent soil volume assuming linear elastic (non-porous) material (Table 1). The interface between the surrounding soil and the anchor block and the improved zone is assumed rigid as a conservative idealisation.

Table 1. Anchor block characteristic material parameters.

Description	γ [kN/m^3]	E [kPa]
Anchor Block	25	30 x 10^6
Improved Zone	21	4.22 x 10^6
Anchor Saddle Block	0	300 x 10^6

3.2 *Fault displacements*

The lateral and vertical displacements are applied to the base of the soil medium at a depth of 100 m resulting in a more intense diversion of the fault rupture path (Anastasopoulos et al. 2008). A lateral fault displacement of 1.0 m as a result of seismic analysis has been modelled by applying 0.5 m movement in y-direction constant with depth to each of the moving blocks in opposite directions. For normal fault movement, a vertical displacement of 0.5 m at a dip angle of 90 degrees to the horizontal has been specified to the base and the vertical boundary of the moving block on the hanging wall while the other half of the base (footwall) displacement boundary remains fixed (see Fig. 3).

3.3 *Ground profile and constitutive model*

The ground profile and the soil parameters used in the PLAXIS 3D model are shown in Table 2. The constitutive model adopted is the elasto-plastic model with standard Mohr-Coulomb (MC) yield surface formulation. The MC model has limitations in terms of modelling soil bifurcation and formation of well-developed shear bands. However, the purpose here is not the determination of the exact location of fault outcrop. Therefore, the simplicity of built-in MC model is chosen over other higher order models.

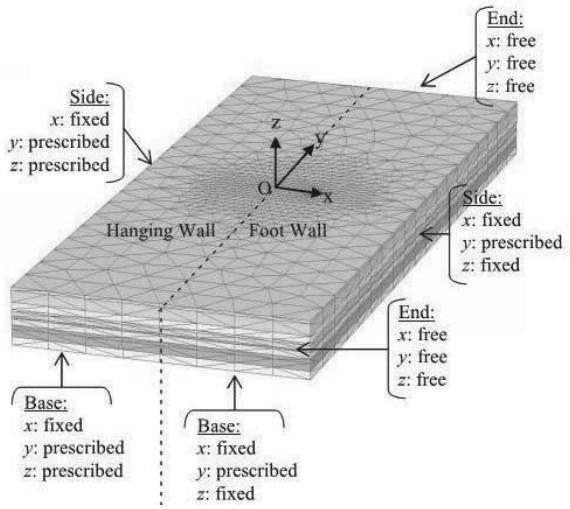

Figure 3.Boundary conditions in PLAXIS 3D model.

As the fault propagation through saturated fine-grained soil deposits occurs too fast for excess pore water pressures to dissipate, the analysis has been performed with undrained conditions in the clay layers using effective parameters for strength and stiffness, which is a method of calculating undrained behaviour by PLAXIS. Drained conditions are assumed in the sand layers. The groundwater level coincides with the existing ground level at -1.7 m.

Table 2. Ground profile and characteristic soil parameters.

Description	Top Level [m]	γ [kN/m^3]	φ'$_{tr}$ [°]	c' [kPa]	E$_{oed}$ [MPa]
Fill	+3	20	35	-	50
SAND	-1.7	18.5	30		15
SAND	-7	19.4	35		52
CLAY	-27.5	19.9	24	9	47
SAND	-39.2	19.9	33.4		47
CLAY	-43	19.9	26	12	60
SAND	-51.5	20.9	35		80
CLAY	-54.7	20.9	26	12	90
SAND	-65.6	20.9	35		80
CLAY	-72.3	20.9	29	24	117
SAND	-86	20.9	35.6		80

K_0 values are equal to 1-sinφ'$_{tr}$.

3.4 *FE mesh*

The large size of the model (700 m along bridge alignment, 1400 m perpendicular to alignment and 130 m vertically) has been a limiting factor for the meshing. The mesh density has been adjusted by creating finer mesh where the anchor block is located. The FE mesh consists of 10-node tetrahedral 3D elements. The number of elements used is 50287 to limit the computing time.

3.5 *Construction sequence*

The construction modelling stages include the calculation of in-situ stresses followed by building the anchor block and applying the structural loads. The last stage is the application of fault displacements.

4 ANALYSIS RESULTS

4.1 *Surface displacements*

Figure 4 shows the free field deformed mesh. The boundary conditions for the large numerical model affect the displacements close to the boundaries but not significantly the displacements around the anchor block. This is because the "cushion" material volumes deform due to the prescribed fault displacement. It is observed that boundary conditions have limited impact on the anchor block thanks to the low-stiffness "cushion". The displacement pattern agrees with typical normal faulting patterns (e.g. Anastasopoulos et al., 2007) as the anchor block follows the movement of the hanging wall.

Figure 5 shows the deformed mesh in a soil-anchor block model. The anchor block moves horizontally due to lateral component of the displacement.

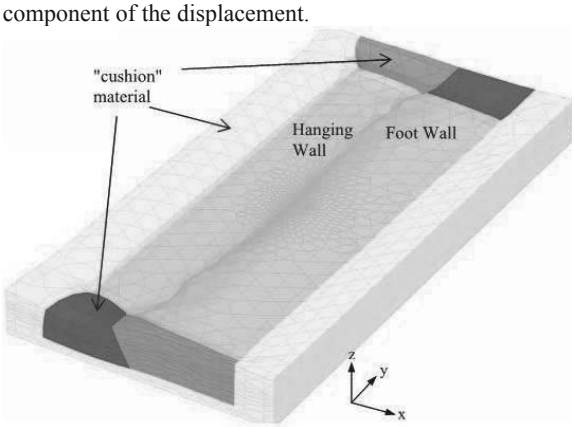

Figure 4. Free-field deformed mesh (scaled up 175 times).

The anchor block shows a forward movement combined with a rotation (see Fig. 5). It is subject to torsion around the z-axis where the lateral fault movement occurs, and y-axis mainly because the block follows the movement of the hanging wall.

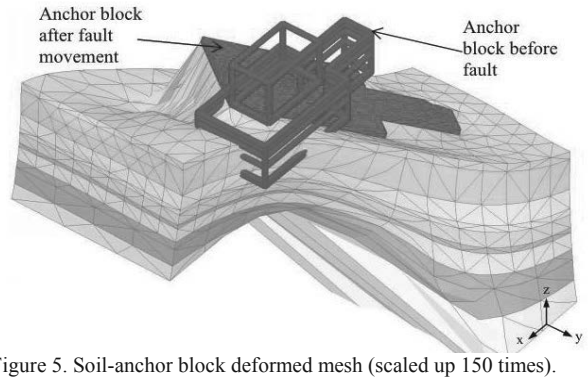

Figure 5. Soil-anchor block deformed mesh (scaled up 150 times).

Figures 6 and 7 present the y- and z-displacement fields at the ground surface, respectively. As a result of fault movement, the anchor block is subjected to maximum differential horizontal (along y-axis) and vertical displacements between the left and right edges of $\Delta u_y = 560$ mm and $\Delta u_z = 490$ mm.

The differential vertical displacement $\Delta u_z = 490$ mm corresponds to the applied vertical fault displacement of 500 mm meaning that the anchor block has a tilt of 1:250 in the direction of the bridge (i.e. x-axis). The rotations of the block around the y- and z-axis are 0.27^o and 0.23^o, respectively. Hence, the vertical displacements as opposed to the horizontal displacements, at the outcrop are transferred directly to the surface. Figures 8 and 9 compare the u_x, u_y and u_z displacements at the ground surface for the free field and the anchor block-soil models along a line in the x-direction passing through the centre of the soil-anchor block.

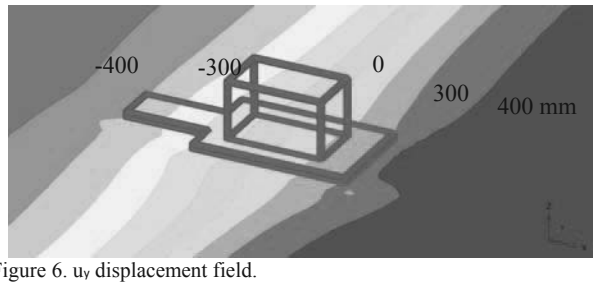

Figure 6. u_y displacement field.

The difference between free-field and the anchor block-soil model displacements at the anchor block boundaries are around $\Delta u_y = 90$ mm and $\Delta u_z = 30$ mm at left corner of the block and $\Delta u_y = 35$ mm and $\Delta u_z = 64$ mm at the right corner of the block.

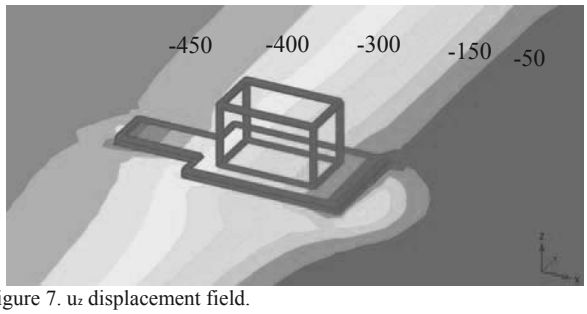

Figure 7. u_z displacement field.

The tilt of the anchor block around the x-axis due to fault movement is approximately 1:1000, which is only 25% of the tilt around the y-axis.

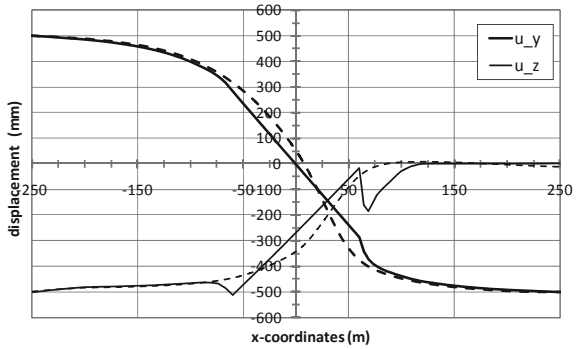

Figure 8. Horizontal (u_y) and vertical (u_z) displacements along the centre of the anchor block at the ground level. Dotted and solid lines represent displacements for free field and soil-anchor block model, respectively.

The discontinuity in vertical downward movement in the vicinity of the right hand side (footwall side) of the block implies separation between the soil and the block developing.

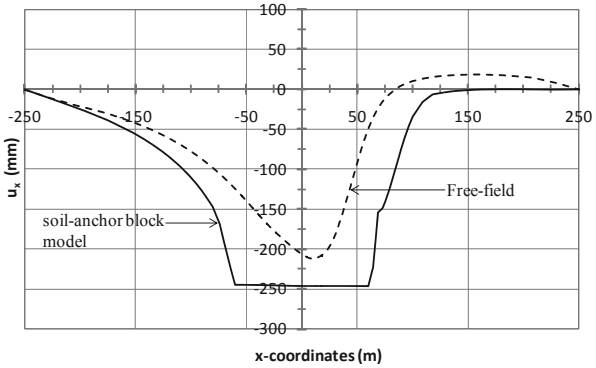

Figure 9. Horizontal displacements, u_x, in the x-direction along the centre of the model at the ground level.

The anchor block also moves 250 mm in the x-direction following the movement of the hanging wall (Fig. 9). The rigid

movement of the anchor block is clearly observed in Figures 8 and 9. It is evident that the rigid anchor block introduces a kinematic constraint to the propagating fault slightly reducing the magnitude of displacements in the y- and z-directions within the footprint of the block in comparison with the free-field motion. The ground moves slightly towards positive x-direction in the footwall side in the free-field model as seen in Figure 9 whereas this does not occur when the anchor block is placed.

4.2 *Horizontal stresses acting on the block*

The effective horizontal normal stresses (σ'_y) acting on the anchor block along the line at x=-55 m and y=10.5 m on the hanging wall are plotted in Figure 10. At this location, it can be observed that the anchor block construction, fill placement and application of the structural loads lead to a stress increase compared to the in-situ stresses. The fault movement increases the stresses further. The final stresses at the chosen location are in general larger than the free-field stresses. Similar tendencies have been observed for sections along the anchor block.

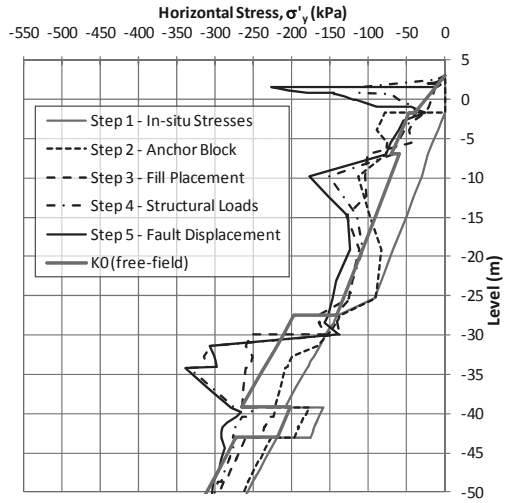

Figure 10. Effective horizontal normal stresses based on construction sequence.

The stresses show rough and irregular patterns due to the unavoidable coarseness of the mesh of this size and the lack of interface elements.

4.3 *Total stresses at the base of the anchor block*

The changes in vertical total stresses at z=-15m due to fault movements are shown in Fig. 11. It can be observed that the fault movement causes an increase of the stresses on the +y sides of the anchor block in the sections x = -55 m and -14 m.

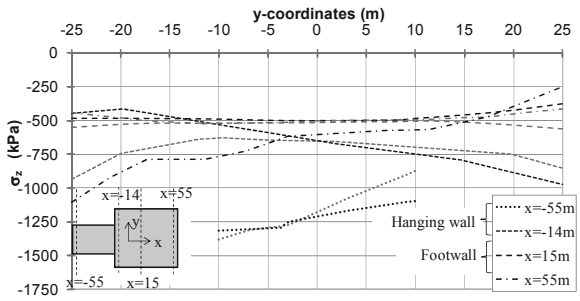

Figure 11. Total vertical stresses at the base of the anchor block before (grey lines) and after (black lines) fault movement.

The opposite behaviour can be observed in the section x=55 m, while no major stress changes occur in the section x=15 m. Due to the anchor block rotations, the vertical stresses at the bottom of the anchor block show a more uneven stress distribution after fault movement.

5 STRUCTURAL IMPLICATIONS

The anchor block only displaces rigidly due to its stiffness. Geometrical changes to the main cable alignment due to the fault-induced anchor block displacement are acceptably small.
The longitudinal inclination and the tilt across the anchor block mean that gravity forces to the cable structures are slightly out of the plane in which they are aligned. However, the gravity load is negligible compared with the cable pull from the suspension bridge.

The only significant effect of the rotation of the anchor block is the slight rotation of the main cables. The plan rotation leads to a sideway sway of the main cable relative to the saddle orientation of the same degree. The anchor block inclination of 1:250 in combination with the 500 mm downward movement and the shortening of the side span result in a slight and negligible roll in the cable saddle. The transverse inclination of the anchor block cross section of 1:1000 is without any significant distortion of the main cable geometry.

6 CONCLUSION

The interaction between oblique-slip fault movement and a suspension bridge anchor block has been investigated using PLAXIS 3D. Innovative boundary modelling has allowed the effects of the fault to be modelled without loss of consistency within a calculation volume of manageable size.

The effect of fault displacements on the horizontal stresses acting on the anchor block side walls is minor. The robust and thick base of the anchor block effectively resists the stress changes on the base of the anchor block due to the fault movement.

7 ACKNOWLEDGEMENTS

The authors gratefully acknowledge the permission by the owner NÖMAYG Joint Venture/Nurol-Özaltın-Makyol-Astaldi-Yüksel-Göçay, and the Contractor IHI Infrastructure Systems CO., Ltd. to publish this paper.

8 REFERENCES

Gazetas G., Anastasopoulos I. and Apostolou M. 2007. Shallow and deep foundations under fault rupture or strong seismic shaking. In *Earthquake Geotechnical Engineering*, Pitilakis (ed), Ch. 9, 185-215, Springer.

Anastasopoulos I., Gazetas G., Bransby M.F., Davies M.C.R and El Nahas A. 2007. Shallow foundation over rupturing normal faults: analysis and experiments, 4th ICEGE, June 25-28,Thessaloniki.

Gazetas G., Pecker A., Faccioli E., Paolucci R. and Anastasopoulos I. 2008. Design recommendations for fault-foundation interaction. *Bulletin of Earthquake Engineering*, 6 (4), 677-687.

Faccioli E., Anastasopoulos I., Gazetas G., Callerio A. and Paolucci R. 2008. Fault rupture–foundation interaction: selected case histories *Bulletin of Earthquake Engineering*, 6 (4), 557-583.

Anastasopoulos I., Gazetas G., Drosos V., Georgarakos T. and Kourkoulis R. 2008. Design of bridges against large tectonic deformation. *Earthquake Engineering & Engineering Vibration*, 7 345-368, 2008.

Loli M., Bransby M.F., Anastasopoulos I., and Gazetas G. 2012. Interaction of caisson foundations with a seismically rupturing normal fault: centrifuge testing versus numerical simulation. *Géotechnique*, 62 (1), 29-44.